RSC Advances

ROYAL SOCIETY
OF **CHEMISTRY**

www.rsc.org/advances

Graphical Abstract

A novel carbazole-phenothiazine dyad small molecule as non-fullerene electron acceptor for polymer bulk heterojunction solar cells

G. D. Sharma, M. Anil Reddy, D. V. Ramana and M. Chandrasekharam

A small organic molecule **CSORG**5 developed as non-fullerene acceptor for bulk heterojunction solar cells. The device based on P3HT:**CSORG**5 (1:1) spin coated from DIO/THF showed high PCE 2.80% compared to spin coated from THF. The PCE has been further increased to 4.16%, when the thin film TiO_2 was inserted between the active layer and Al electrode.

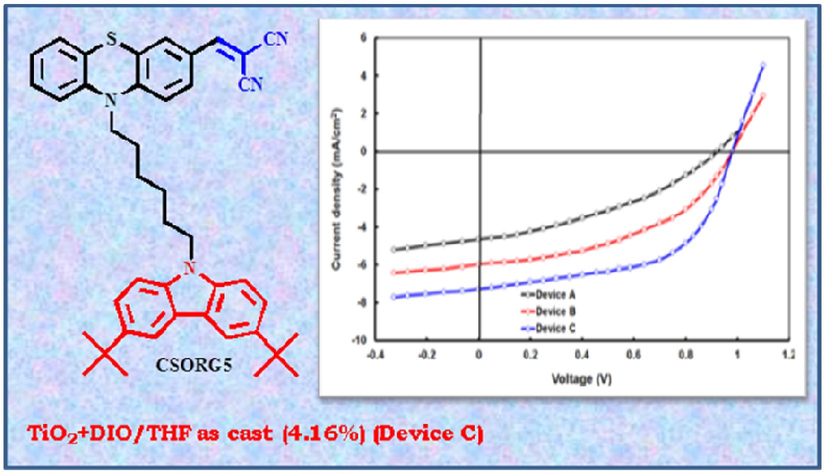

A novel carbazole-phenothiazine dyad small molecule as non-fullerene electron acceptor for polymer bulk heterojunction solar cells

G. D. Sharma,[a*] M. Anil Reddy,[b] D. V. Ramana,[b] M. Chandrasekharam[b*]

[a]R & D center for Science and Engineering, JEC group of Colleges, Jaipur Engineering College Campus, Kukas, Jaipur- 303101, India

[b]Network of Institutes for solar energy, Inorganic & Physical Chemistry Division, CSIR-Indian Institute of Chemical Technology, Uppal Road, Tarnaka, Hyderabad -500607, India

Abstract:

A new organic small molecule, 2-((10-(6-(3,6-di-tert-butyl-9H-carbazol-9-yl)hexyl)-10H-phenothiazin-7-yl)methylene) malononitrile named as **CSORG**5 has been synthesized and successfully applied for organic bulk heterojunction (BHJ) solar cells as a novel electron acceptor along with P3HT as donor. **CSORG**5 molecule possess facile synthesis, solution processability, visible light absorption, a properly matched lowest unoccupied molecular orbital (LUMO) energy level with conjugated polymers and moderate electron mobility, making the molecule ideal acceptor for P3HT and other low band gap conjugated polymers. The BHJ organic solar cell constructed from P3HT:**CSORG**5 (1:1) active layer processed from DIO/THF solvent, exhibit a high open circuit voltage up to 0.98 V resulting over all power conversion efficiency of 2.80%. Further, the PCE has been enhanced up to 4.16% when a thin layer of TiO_2 is inserted in between the active layer and Al electrode.

Keywords: Non-fullerene acceptor, bulk heterojunction solar cells, optical spacer, power conversion efficiency

* Corresponding authors e-mail: csmalapaka@yahoo.com (MC) and gdsharma273@gmail.com (GDS)

Introduction:

Among various photovoltaic technologies, organic solar cells garnered immense attention because of its low cost, flexibility, chemical versatility and easy fabrication compared to other alternative solar cell technologies.[1] Much effort has been paid in improving the power conversion efficiency of typical polymer/fullerene based bulk heterojunction (BHJ) organic solar cells up to 10%,[2] where in, the fullerenes as acceptor are playing key role. The most common acceptor materials that are usually employed in BHJ organic solar cells are phenyl-C_{61}-butyric acid methyl ester ($PC_{61}BM$) and phenyl-C_{71}-butyric acid methyl ester ($PC_{71}BM$) owing to their large electron affinity and strong tendency to accepts the electron from the donor semiconductors, ability to form favorable nanoscale networks with donor conjugated polymers and high electron mobility.[3] However the efficacy of fullerenes as acceptors was hampered by its weak absorption in the visible region and near IR-region, limited tunable HOMO and LUMO energy levels and expensive synthesis and purification procedures are the barrier to commericialization.[4] In order to circumvent these drawbacks, it is highly desirable to develop new fullerene free acceptor materials, which exhibit favorable electron transport properties and broad absorption over the visible region of solar spectrum and bandgap tunability. Recently, some non-fullerene acceptors have been developed and a few materials showed efficiency over 2%.[5] More recently, J. Pei *et al.* have reported PCE in the range of 2.11-2.90%, on fluoranthene fused imide derivatives based electron acceptors in solution processed inverted bulk hetero junction solar cells with P3HT as a donor.[6] J. Yao *et al.* have reported high PCE 4.03%, on perylene diimide dimer-based non fullerene acceptor material for efficient solution processed BHJ solar cells.[7a] Recently, BHJ organic solar cells based on solution processed non-fullerene acceptors have shown PCE up to 4 % .[7b]

Phenothiazine is a common heterocyclic compound acquiring electron rich nitrogen and sulphur hetero atoms and is known to depress the molecular aggregation due to its non-planarity.[8a-8d] Owing to the unique optical and electrochemical properties, phenothiazine based supramolecules have been widely utilized in organic light emitting diodes (OLEDs), photovoltaic cells and organic thin film transistors. In continuation of our pursuits in the synthesis and application of phenothiazine based ruthenium and metal-free sensitizers for dye sensitized solar cells, we are interested in the development of phenothiazine based small molecules for organic photovoltaic applications.[8e-8g]

As a part of our ongoing research program, we have been engaged to develop new materials for DSSC[8e-8g, 9] and OSCs.[10] In this paper, we report synthesis and characterization of non-fullerene electron acceptor material **CSORG5** and its application in solution processed OSC as acceptor. **CSORG**5 compound is a phenothiazine connected via a hexyl chain with a di-*tert* butyl carbazole unit, wherein the alkyl chain can improve the solubility. While the extra electron donor, di-*tert*-butyl carbazole unit can contribute to improvement in the molar extinction coefficient and, the malononitrile acts as good electron acceptor. The novel small molecule exhibited broad band absorption complementary to P3HT, appropriate energy levels matching with P3HT and moderate electron mobility. After optimization of processing of active layer, solution processed BHJ OSCs based on P3HT:**CSORG**5 (spin cast from DIO/THF) showed PCE as high as 2.80%, which is further improved up to 4.16%, when a thin layer of TiO_2 was deposited in between active layer and Al electrode.

Experimental section

Materials and Instruments

The starting materials phenothiazine, carbazole, dibromohexane and malononitrile were purchased from sigma-aldrich. The solvents were purified by standard procedures and purged with nitrogen before use. All other chemicals used in this work were analytical grade and were used without further purification. All the reactions were performed under argon atmosphere unless and otherwise mentioned. Chromatographic separations were carried out on silica gel (60-120 mesh). **^{1}H NMR, ^{13}C NMR** spectra were recorded on **Avance 300 and 500 MHz** spectrometer using TMS as internal standard. Mass spectra were recorded on Shimadzu LCMS-2010EV model with ESI probe. Absorption spectra were recorded on a shimadzu UV-Vis to near IR 3600 spectrometer. Electrochemical data were recorded using Autolab potentiostat/ Galvanostat PGSTAT30. The cyclic voltammogram curves were obtained from a three electrode cell in 0.1 M Bu_4NPF_6 tetrahydrofuran solution at a scan rate of 100 mV s^{-1}, Pt wire as a counter electrode, Pt rod as a working electrode and *NHE* as reference electrode and calibrated with ferrocene.

Device fabrication and characterization

The solar cells were fabricated on an indium doped tin oxide (ITO) coated glass substrate with a structure ITO/PEODT:PSS/P3HT:**CSORG**5/Al. The ITO coated glass substrates were first cleaned with detergent, ultra-sonicated in acetone and isopropyl alcohol, and subsequently dried overnight in an oven. A thin layer poly(3,4-ethylene dioxythiophe-ne):poly(styrene sulfonate) (PEDOT:PSS) (Aldrich) of thickness 60 nm was spin coated from aqueous solution onto the top of ITO glass substrate and baked for 10 min at 120 °C in air. The solutions of P3HT (5 mg ml^{-1}) and **CSORG**5 (5 mg ml^{-1}) in either THF or DIO/THF were prepared and mixed by blending P3HT:**CSORG**5 in 1:1 ratio. The active layer was formed by spin coating the blend solution (1500 rpm for 25 s) onto the top of PEDOT:PSS layer, immediately covering with a Petri dish until dry. The dried substrates were then baked at 60 °C for 10 min before depositing the metal electrode. The metal contact was thermally deposited under vacuum on the top of active layer. The device area (0.25 cm^2) was formed by the overlap between the deposited metal and the ITO layer. For the device with TiO_2 layer, the thin TiO_2 layer was deposited on the top of the active layer from a sol gel paste and dried in ambient conditions at a temperature 60° C for 30 min, before the deposition of final aluminum (Al) electrode through thermal evaporation. Photovoltaic cells without protective encapsulation were subsequently tested AM1.5 G irradiation with illumination intensity using a solar simulator coupled with AM1.5 optical filter. The current-voltage (J-V) characteristics of the devices were recorded using a Keithley source meter (model 2400). The incident photon to current conversion efficiency (IPCE) of the devices was measured using a monochromator and xenon lamp as light source and resulting photocurrent was measured with source meter under short circuit condition.

Synthesis

2-((10-(6-(3,6-di-tert-butyl-9H-carbazol-9-yl)hexyl)-10H-phenothiazin-7-yl)methylene)malononitrile (CSORG5):

A 25 ml flask was charged with Compound **3** (110 mg, 0.186 mmol) in $CHCl_3$ (8 mL), malononitrile (25 mg, 0.373 mmol) and piperidine (0.061 mL, 0.616 mmol). The mixture was refluxed for 8 h. After cooling to room temperature, 2 M aqueous HCl (5 mL) was added and the contents were stirred for 30 min. Then the mixture was washed with water and extracted three times with chloroform. The combined organic fractions were washed with brine and dried over Na_2SO_4. The solvent was removed under reduced pressure and the residue purified by column chromatography using methanol/dichloromethane (1/9; v/v) as eluent to afford **CSORG**5 (72%) as dark red powder. Mp 176-178 °C. **^{1}H NMR** (300 MHz, $CDCl_3$, δ): 8.02 (s, 2H), 7.69 (d, 1H), 7.38-7.42 (m, 4H), 7.17 (d, 2H), 7.03-7.09 (m, 2H), 6.92-6.97 (m, 1H), 6.73 (t, 2H), 4.21 (t, 2H), 3.78 (t, 2H), 1.72-1.86 (m, 4H), 1.45 (s, 18H), 1.36 (broad, 4H). **^{13}C NMR** (75 MHz, $CDCl_3$, δ): 157.232, 150.621, 142.324, 141.473, 138.834, 131.283, 129.395, 127.749, 127.582, 125.096, 124.988, 124.127, 123.199, 122.572, 116.239, 116.004, 114.828, 114.596, 113.468, 107.897, 47.835, 42.809, 34.607, 32.026, 29.023, 26.834, 26.518, 26.427. **FT-IR**(**KBr**) cm^{-1}: 2955, 2929, 2866, 2219, 1601, 1561, 1468, 1443, 1406, 1363, 1325, 1296, 1256, 1223, 1189, 1161, 1103, 1032, 936, 876, 814, 750, 646, 609, 463. **ESI-MS** calcd for $C_{42}H_{44}N_4S$ 636, found 659 $(M+Na)^+$. Anal. Calcd for $C_{42}H_{44}N_4S$: C, 79.21; H, 6.96; N, 8.80; S, 5.03. Found: C, 78.41; H, 5.89; N, 9.13; S, 5.63.

Results and discussion

General synthesis

The synthetic route of **CSORG**5 is shown in scheme 1. Compounds **1**, **2** and **3** were synthesized by our previous reports.[8] The product **3** was subjected to Knoevenagel condensation with malononitrile in the presence of piperidine using chloroform as a solvent, to give corresponding compound **CSORG**5 with 72% yield.

Optoelectronic properties

Figure 1 shows the absorption spectra of **CSORG**5 in THF solution and thin film. In solution, **CSORG**5 exhibited strong absorption with the maximum absorption coefficient of 1.85×10^4 and 1.69×10^4 M^{-1} cm^{-1} at 330 nm and 455 nm, respectively. The thin film of **CSORG**5 shows significant broad absorption bands throughout 300 to 550 nm, relatively to that in solution with absorption peaks at 330 nm and 470 nm. In thin film, the longer wavelength absorption band was red shifted by 15 nm relative to that in solution and the optical band gap estimated from its absorption edge (565 nm) is 2.19 eV.

The oxidation and reduction potentials of **CSORG**5 were calculated from the cyclic voltammetry (CV) measured in THF solvent and the cyclic voltammogram is shown in Figure 2. As shown in Figure 2, **CSORG**5 exhibits irreversible oxidation and quasi-reversible oxidation waves. The onset oxidation and reduction potential *vs* NHE are 0.88 V and -1.32 V, respectively. The HOMO and LUMO energy levels were estimated to be -5.58 eV and 3.40 eV from the onset oxidation and reduction potential, respectively, assuming the absolute energy level of NHE to be 4.7 eV below vacuum level. The HOMO and LUMO energy levels are lower than those for P3HT (-4.95 eV and -3.00 eV).[11] The difference in LUMO (0.40 eV) and HOMO (0.63 eV) between the **CSORG**5 and P3HT are sufficient enough for the efficient excitons dissociation.[12] Moreover, the difference between the HOMO of P3HT and LUMO of **CSORG**5 is as large as 1.55 eV, which may results high V_{oc} for polymer BHJ solar cells using P3HT and **CSORG**5 as electron donor and acceptor, respectively.

Photovoltaic properties

The current-voltage characteristics of the two devices using **CSORG**5:P3HT (1:1 weight ratio) BHJ active layer (device A as cast from THF and device B cast from DIO (3% vol) / THF) are shown in Figure 3 and the corresponding photovoltaic parameters *i.e.*, short circuit photocurrent (J_{sc}), open circuit voltage (V_{oc}), fill factor (FF) and power conversion efficiency are complied in table 1. The blend ratio with 1:1 wt shows best photovoltaic response with J_{sc} = 4.65 mA/cm^2, V_{oc} = 0.92 V, FF = 0.41 and PCE = 1.75% (device A). The device showed quite high V_{oc} as compared to devices based on PCBM acceptor which is attributed to the large difference between the LUMO level of **CSORG**5 and HOMO level of P3HT. When the active layer was spin coated from DIO/THF (device B) the J_{sc}, V_{oc} and FF showed improvements up to 5.96 mA/cm^2, 0.98 V and 0.48, respectively, leading to the PCE about 2.80%, a 60% enhancement as compared to that for device A. There is a significant increase in the V_{oc} for the device based on solvent additive active layer as compared to counterpart device cast from THF solvent. The adsorbed high boiling point solvent additive *i.e.* DIO may render relaxation and self organization of the molecules, which promotes the intermolecular interaction and ordered packing[13] and thus reduces defects and series resistance in film, resulting improvement in V_{oc}.[14] As the low value of J_{sc} using **CSGOR**5 as acceptor is low as compared to that with PCBM may be attributed to the higher value of LUMO level as compared to PCBM, forming a barrier for electron collection at cathode.

The incident photon to current conversion efficiency (IPCE) spectra of these three devices is shown in Figure 4. These devices show broad plateau of IPCE spectra from 425 nm to 650 nm and closely resemble to the absorption bands of both **CSORG**5 and P3HT indicating both **CSORG**5 and P3HT are contributing to the photocurrent generation. The IPCE values for the device B are higher than that for the device A may be due to the increase in the crystallization of P3HT with the addition of solvent additive as reported in literature.[15]

The hole and electron mobilities in the BHJ active layer were measured by a space charge limited current (SCLC) method with device structure ITO / PEDOT:PSS / P3HT:**CSORG**5 / Au and Al/ P3HT:**CSORG**5/Al, respectively. The average hole and electron mobility for the blend cast from THF only were found to be about 8.9 x10^{-5} cm^2/Vs and 1.2 x10^{-6} cm^2/Vs, respectively. But when the BHJ active layer was cast from DIO/THF, the hole mobility improves up to 1.2 x10^{-4} cm^2/Vs and electron mobility also increases 3.4 x10^{-5} cm^2/Vs. The better charge transport is beneficial for the enhancement of J_{sc}, therefore the device B showed higher J_{sc} in comparison to device A. The electron/hole mobility ratio for device A and B are about 0.014 and 0.28, respectively. The improvement in the electron /hole mobility ratio for device B as compared to device A indicates the more balanced charge transport in device B is responsible for the increase in J_{sc} and FF.

The PCE of organic solar cell (device B) is still low and may be due to the mismatch between the optical absorption length and insufficient charge transport in the device.[16] The optical absorption can be increased by increasing the thickness of the BHJ active layer, but this increases the probability of charge recombination that can decrease the carrier drift velocity by reducing the internal electric field. Therefore, proper structuring of the solution processed organic solar cell needed to increase the light harvesting within the thin active layer is very important. It has been reported that the light absorption can be enhanced by altering the spatial distribution of the optical electric field inside the device.[17] It is well known that the optical interference between the incident and back reflected light, the intensity of the light at the surface of the metal electrode is zero. Therefore, the insertion of the optical spacer between the active layer and metal electrode can increase the optical absorption of the active layer. We have inserted a thin layer of TiO_2 in between the active layer and metal electrode for device C. Figure 3 also shows the current-voltage characteristics under illumination of the devices, with and without TiO_2 layer and the photovoltaic parameters are compiled in table 1. The J_{sc} and FF increase from 5.96 mA/cm^2 and 0.48 to 7.28 mA/cm^2 and 0.56 respectively, enhancing the over PCE from 2.80% to 4.16%. To understand the enhancement in J_{sc}, we have recorded the optical absorption of the active layer before and after the insertion of TiO_2 layer and shown in Figure 5. It can be seen from Figure 5 that the absorption of the active layer between 350–700 nm increases with the incorporation of the TiO_2 layer. The enhancement in the IPCE spectra of the device with TiO_2 layer (Figure 4), in this wavelength region is in good agreement with the increase in absorption of active layer. The enhancement in both absorption and IPCE leads to an increase in the J_{sc} and overall PCE.

We have also determined the maximum photo-induced carriers generation rate (G_{max}) in the BHJ solar cells with and without TiO_2 layer. Figure 6a shows the effect of TiO_2 optical spacer on the photocurrent density (J_{ph}) versus the internal voltage (V_{in}) of the device with and without TiO_2 layer under illumination. J_{ph} was calculated as $J_{ph} = J_L - J_d$, where J_L and J_d are the current density under illumination and in dark, respectively,[18] V_{in} is determined as $V_{in} = V_{bi} - V_{appl}$, where V_{bi} is the built in voltage, which refer to the voltage at which J_{ph} is zero, and V_{appl} is the applied voltage.[19] As can be seen from figure 6a that J_{ph} increases with the V_{in} at low voltage but J_{ph} saturates at high voltage (1.8 V). At high voltages, the internal field is large enough to sweep out all the charge carriers to the electrodes and the saturated photocurrent (J_{phmax}) is limited only by the number of absorbed photons, can be expressed as

$$J_{phsat} = qLG_{\max} \text{ ----------- } (1)$$

Where q is electronic charge, L is the thickness of the active layer and G_{max} is the maximum photo-induced carrier generation rate per unit volume.[20] The value of G_{max} for the device without and with TiO_2 layer is 4.18 x10^{26} m^{-3}/s (J_{phmax} = 6.03 mA/cm^2) and 5.45 x10^{26} m^{-3}/s (J_{phmmax}= 7.85 mA/cm^2), respectively. These values show that the G_{max} increases after the insertion of optical spacer. Since the G_{max} corresponds to the maximum number of photons absorbed by the active layer, such enhancement indicates that the absorption of light increases in the device with the incorporation of TiO_2 in between the active layer and Al electrode.

The charge collection efficiency (P_c) is also a deciding factor for the PCE of an organic solar cell. We have also investigated the charge collection behavior in the devices with and without TiO_2 layer. The J_{ph} of the solar cell can be written as[18, 21]

$$J_{ph} = qLG_{\max}P_c \text{ ------------------------ (2)}$$

where P_c is the charge collection efficiency. From above eqs (1) and (2), we have calculated the P_c by normalizing the J_{ph} with J_{phsat} i.e (J_{ph}/J_{phsat}). Figure 6b shows the charge collection probability (P_c) with respect to V_{in} under illumination intensity of 100 mW/cm^2. As shown in Figure 6b that the value of P_c for device with TiO_2 optical layer is higher than that for the device without TiO_2. Therefore the TiO_2 optical spacer increases both the light absorption and charge collection, thereby increasing the J_{sc}. As can be seen from the current-voltage characteristics of the devices in dark (Figure 7), the TiO_2 layer effectively reduces the leakage current in the reverse bias. The leakage current is due to the recombination of the charge carriers in the device and therefore the insertion of TiO_2 effectively reduces the charge recombination.

To get more information about the effect of TiO_2 layer on the charge recombination mechanism in the device, we have measured the J_{sc} at different illumination intensities. The variation of J_{sc} with the illumination intensity in log-log scale is shown in Figure 8. A power law dependence of J_{sc} upon the illumination intensity is generally observed in organic solar cells and can be expressed as

$$J_{sc} \propto I^{\gamma} \text{ -------------------- (3)}$$

Where I is the illumination intensity and γ is the exponential factor.[18, 20a, 22] The data shown in Figure 8 were fitted to power law using eq (3), we found the value of γ about 0.89 and 0.93, for the device without and with TiO_2 layer, respectively. The higher value of exponential factor for the device with TiO_2 layer than that for without TiO_2 layer, indicates that bimolecular recombination is reduced for this device.[23] This result agrees with an increase in charge collection efficiency and fill factor by inserting the TiO_2 layer.

We have also measured the electron and hole mobility of the devices using the P3HT:**CSORG5** (DIO/THF cast)/TiO_2, and found that the electron and hole mobilities are about

7.4×10^{-5} cm^2/Vs and 1.8×10^{-4} cm^2/Vs, respectively. The ratio of electron/hole mobility improves to 0.41 as compared to device B. The improvement in this ratio is also an indication of the reduction in recombination. As the conduction band edge of TiO_2 is very close to the work function to Al cathode electrode, the collection of the electrons also improved for device C as compared to device B.

Conclusion

In summary, a novel D-A solution processed small molecule **CSORG**5 was developed as electron acceptor for polymer BHJ solar cells. It exhibits broad absorption spectra complementary to that P3HT and suitable HOMO and LUMO for efficient exciton dissociation. The BHJ solar cell based on P3HT:**CSORG**5 (1:1) active layer spin coated with DIO/THF solvent showed higher PCE about 2.80% as compared to the device processed from the THF solvent (PCE = 1.75%). The more balance charge transport is attributed to the higher value of J_{sc} and PCE for the device processed with DIO/THF solvent. The PCE has been further improved up to 4.16%, when a thin film of TiO_2 layer was inserted in between the active layer and Al electrode. The incorporation of the TiO_2 layer increases the charge collection efficiency due to the more balanced charge transport.

Acknowledgements

MAR thanks to CSIR-New Delhi for senior research fellowship. We acknowledge useful discussions with Dr V. Jayathirtha Rao and financial help from project no. NWP-0054.

References

1. G. Yu, J. Gao, J. C. Hummelen, F. Wudl and A. J. Heeger, *Science*, 1995, **270**, 1789-1791.
2. (a) J. You, L. Dou, K. Yoshimura, T. Kato, K. Ohya, T. Moriarty, K. Emery, C.-C. Chen, J. Gao and Y. Yang, *Nat. Commun.*, 2013, **4**, 1-10; (b) Z. He, C. Zhong, S. Su, M. Xu, H. Wu and Y. Cao, *Nat. Photonics*, 2012, **6**, 591-595.
3. (a) J. C. Hummelen, B. W. Knight, F. LePeq and F. Wudl, *J. Org. Chem.*, 1995, **60**, 532-538; (b) M. M. Wienk, J. M. Kroon, W. J. H. Verhees, J. Knol, J. C. Hummelen, P. A. van Hal and R. A. J. Janssen, *Angew. Chem. Int. Ed.*, 2003, **42**, 3371-3375; (c) Y. F. Li,

Acc. Chem. Res., 2012, **45**, 723-733; (d) F. G. Brunetti, X. Gong, M. Tong, A. J. Heeger and F. Wudl, *Angew. Chem. Int. Ed.*, 2010, **49**, 532-536; (e) F. G. Brunetti, R. Kumar and F. Wudl, *J. Mater. Chem.*, 2010, **20**, 2934-2948.

4. (a) Y. J. He and Y. F. Li, *Phys. Chem. Chem. Phys.*, 2011, **13**, 1970-1983; (b) M. Lenes, S. W. Shelton, A. B. Sieval, D. F. Kronholm, J. C. Hummelen and P. W. M. Blom, *Adv. Funct. Mater.*, 2009, **19**, 3002-3007. (c) P. Sonar, J. P. F. Lim and K. L. Chan, *Energy Environ. Sci.*, 2011, **4**, 1558-1574.
5. (a) Y. Lin, P. Cheng, Y. Li and X. Zhan, *Chem. Commun.*, 2012, **48**, 4773-4775; (b) J. E. Anthony, *Chem. Mater.*, 2011, **23**, 583-590; (c) G. D. Sharma, M. S. Roy, J. A. Mikroyannidis and K. R. Justin Thomas, *Org. Electron.*, 2012, **13**, 3118-3129; (d) X. Zhao, C. Piliego, B. Kim, D. A. Poulsen, B. Ma, D. A. Unruh and J. M. J. Fréchet, *Chem. Mater.*, 2010, **22**, 2325-2332; (e) Qifan Yan, Yan Zhou, Yu-Qing Zheng, Jian Pei and Dahui Zhao, *Chem. Sci.*, 2013, **4**, 4389-4394; (f) Yan Zhou, Lin Ding, Ke Shi, Ya-Zhong Dai, Na Ai, Jian Wang and Jian Pei, *Adv. Mater.*, 2012, **24**, 957-961; (g) Yuze Lin, Yongfang Li, Xiaowei Zhan, Adv. Energy Mater., 2013, **3**, 724-728; (h) Y. Lin, X. Zhan, Mater. Horiz. DOI:10.1039/c4mh00042k.
6. Yan Zhou, Ya-Zhong Dai, Yu-Qing Zheng, Xiao-Ye Wang, Jie-Yu Wang and Jian Pei, *Chem. Commun.*, 2013, **49**, 5802-5804.
7. (a) X. Zhang, Z. Lu, L. Ye, C. Zhan, J. Hou, S. Zhang, B. Jiang, Y. Zhao, J. Huang, S. Zhang, Y. Liu, Q. Shi, Y. Liu, J. Yao, *Adv. Mater.*, 2013, **25**, 5791-5797; (b) D. Mori, H. Benten, I. Okada, H. Ohkita, S. Ito, *Adv. Energy Mater.*, 2014, **4**, DOI: 10.1002/aenm.201301006.
8. (a) M.-J. Kim, Y.-J. Yu, J.-H. Kim, Y.-S. Jung, K.-Y. Kay, S.-B. Ko, C.-R. Lee, I.-H. Jang, Y.-U. Kwon and N.-G. Park, *Dyes Pigm.*, 2012, **95**, 134-141; (b) H. Tian, X. Yang, R. Chen, Y. Pan, L. Li, A. Hagfeldt and L. Sun, *Chem. Commun.*, 2007, 3741-3743; (c) S. H. Kim, H. W. Kim, C. Sakong, J. Namgoong, S. W. Park, M. J. Ko, C. H. Lee, W. I. Lee and J. P. Kim, *Org. Lett.*, 2011, **13**, 5784-5787; (d) M. Cheng, X. Yang, F. Zhang, J. Zhao and L. Sun, *J. Phys. Chem. C*, 2013, **117**, 9076-9083; (e) G. Marotta, M. A. Reddy, S. P. Singh, A. Islam, L. Han, F. D. Angelis, M. Pastore and M. Chandrasekharam, *ACS Appl. Mater. Interfaces*, 2013, **5**, 9635-9647; (f) M. Chandrasekharam, G. Rajkumar, Ch. Srinivasa Rao, T. Suresh and P. Y. Reddy, *Syn. Metals*, 2011, **161**, 1469-1476; (g) S.

Agrawal, M. Pastore, G. Marotta, M. Anil Reddy, M. Chandrasekharam and F. De Angelis, *J. Phys. Chem. C*, 2013, **117**, 9613-9622.

9. (a) Maria Grazia Lobello, Kuan-Lin Wu, Marri Anil Reddy, Gabriele Marotta, Michael Grätzel, Mohammad K. Nazeeruddin, Yun Chi, Malapaka Chandrasekharam, Giuseppe Vitillaro, Filippo De Angelis, *Dalton Trans*., 2014, **43**, 2726-2732; (b) M. Chandrasekharam, T. Suresh, S.-P. Singh, B. Priyanka, K. Bhanuprakash, A. Islam, L. Han, M. Lakshmi Kantam, *Dalton Trans*., 2012, **41**, 8770-8772; (c) M. Chandrasekharam, M.-A. Reddy, S.-P. Singh, B. Priyanka, K. Bhanuprakash, M. Lakshmi Kantam, A. Islam, L. Han, *J. Mater. Chem*., 2012, **22**, 18757-18760.
10. (a) G. D. Sharma, M. Anil Reddy, K. Ganesh, Surya Prakash Singh, M. Chandrasekharam, *RSC Adv*., 2014, **4**, 732-742; (b) M. Chandrasekharam, M. Anil Reddy, K. Ganesh, Surya Prakash Singh, G. D. Sharma, *Org. Electronics*, 2014, **15**, 2116-2125.
11. John A. Mikroyannidis, Antonis N. Kabanakis, S. S. Sharma and G. D. Sharma, *Adv. Funct. Mater*., 2011, **21**, 746-755.
12. C. J. Brabec, C. Winder, N. S. Sariciftci, J. C. Hummelen, A. Dhanabalan, P. A. van Hal and R. A. J. Janssen, *Adv. Funct. Mater*., 2002, **12**, 709-712.
13. G. Li, V. Shrotriya, J. Huang, Y. Yao, T. Moriarty, K. Emery and Y. Yang, *Nat. Mater*., 2005, **4**, 864-868.
14. (a) B. Qi and J. Wang, *J. Mater. Chem*., 2012, **22**, 24315-24325; (b) D. Credgington and J. R. Durrant, *J. Phys. Chem. Lett*., 2012, **3**, 1465-1478; (c) Yuze Lin, Yongfang Li and Xiaowei Zhan, *Adv. Energy Mater*., 2013, **3**, 724-728.
15. J. K. Lee, W. L. Ma, C. J. Brabec, J. Yuen, J. S. Moon, J. Y. Kim, K. Lee, G. C. Bazan and A. J. Heeger, *J. Am. Chem. Soc*., 2008, **130**, 3619-3623.
16. (a) H. A. Atwater and A. Polman, *Nat. Mater*., 2010, **9**, 205-213; (b) G. Dennler, M. C. Scharber and C. J. Brabec, *Adv. Mater*., 2009, **21**, 1323-1338; (c) J. Peet, A. J. Heeger and G. C. Bazan, *Acc. Chem. Res*., 2009, **42**, 1700-1708.
17. (a) L. A. A. Pettersson, L. S. Roman and O. Inganas, *J. Appl. Phys*., 1999, **86**, 487-496; (b) J. Y. Kim, S. H. Kim, H.-H. Lee, K. Lee, W. Ma, X. Gong and A. J. Heeger, *Adv. Mater*., 2006, **18**, 572-576; (c) J. Gilot, I. Barbu, M. M. Wienk and R. A. J. Janssen, *Appl. Phys. Lett*., 2007, **91**, 113520(1)-113520(3); (d) A. Roy, S. H. Park, S. Cowan, M. H.

Tong, S. Cho, K. Lee and A. J. Heeger, *Appl. Phys. Lett.*, 2009, **95**, 013302(1)-013302(3).

18. S. R. Cowan, A. Roy and A. J. Heeger, *Phys. Rev. B*, 2010, **82**, 245207(1)- 245207(10).
19. S. R. Cowan, R. A. Street, S. Cho and A. J. Heeger, *Phys. Rev. B*, 2011, **83**, 035205(1)-035205(8).
20. (a) V. D. Mihailetchi, H. X. Xie, B. de Boer, L. J. A. Koster and P. W. M. Blom, *Adv. Funct. Mater*., 2006, **16**, 699-708; (b) V. D. Mihailetchi, L. J. A. Koster, J. C. Hummelen and P.W. M. Blom, *Phys. Rev. Lett*., 2004, **93**, 216601(1)- 216601(4).
21. R. A. Street, S. Cowan and A. J. Heeger, *Phys. Rev. B*, 2010, **82**, 121301(1)- 121301(4).
22. I. Riedel, J. Parisi, V. Dyakonov, L. Lutsen, D. Vanderzande and J. C. Hummelen, *Adv. Funct. Mater*., 2004, **14**, 38-44.
23. (a) P. Schilinsky, C. Waldauf and C. J. Brabec, *Appl. Phys. Lett*., 2002, **81**, 3885-3887; (b) J. K. J. Van Duren, X. Yang, J. Loos, C. W. T. Bulle-Lieuwma, A. B. Sieval, J. C. Hummelen and R. A. J. Janssen, *Adv. Funct. Mater*., 2004, **14**, 425-434.

Table 1: Photovoltaic parameters of device A, B and C.

Device	J_{sc} (mA/cm^2)	V_{oc} (V)	FF	PCE (%)	$\mu_e/\ \mu_h$
A	4.95	0.92	0.41	1.75	0.014
B	5.96	0.98	0.56	2.80	0.28
C	7.28	0.98	0.56	4.16	0.41

Scheme 1: Synthetic route for **CSORG**5

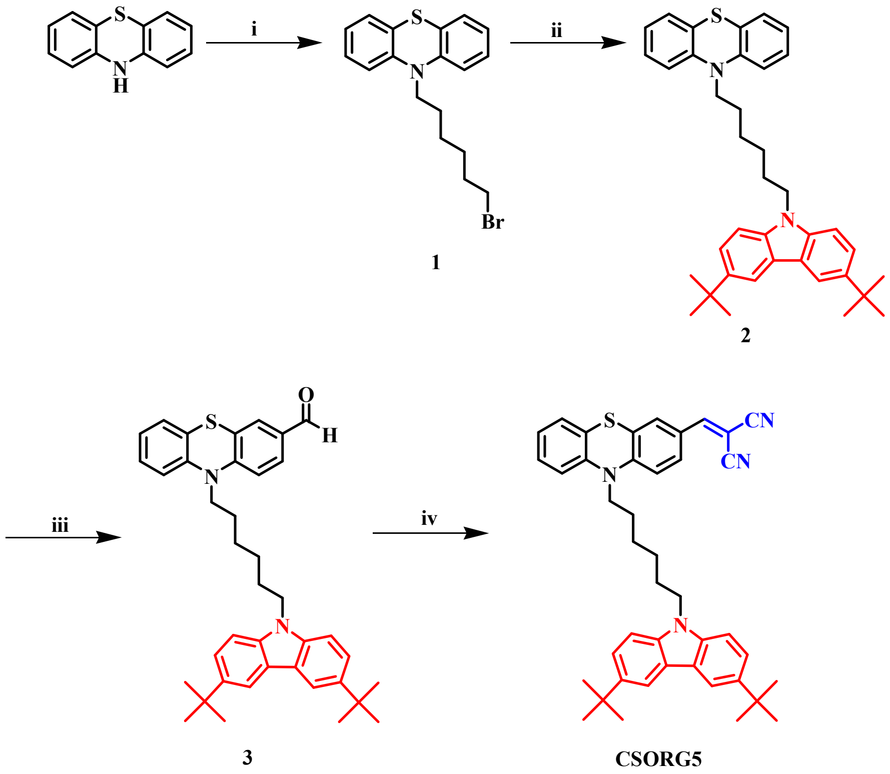

Reagents & conditions: (i) NaH, DMF, 1, 6-dibromohexane, RT, overnight (ii) KOH, DMF, di-*tert*-butyl carbazole, RT, 6 hrs (iii) DMF, $POCl_3$, 1, 2-dichloroethane, reflux, overnight (iv) Piperidine, $CHCl_3$, Malononitrile, reflux, 8hrs.

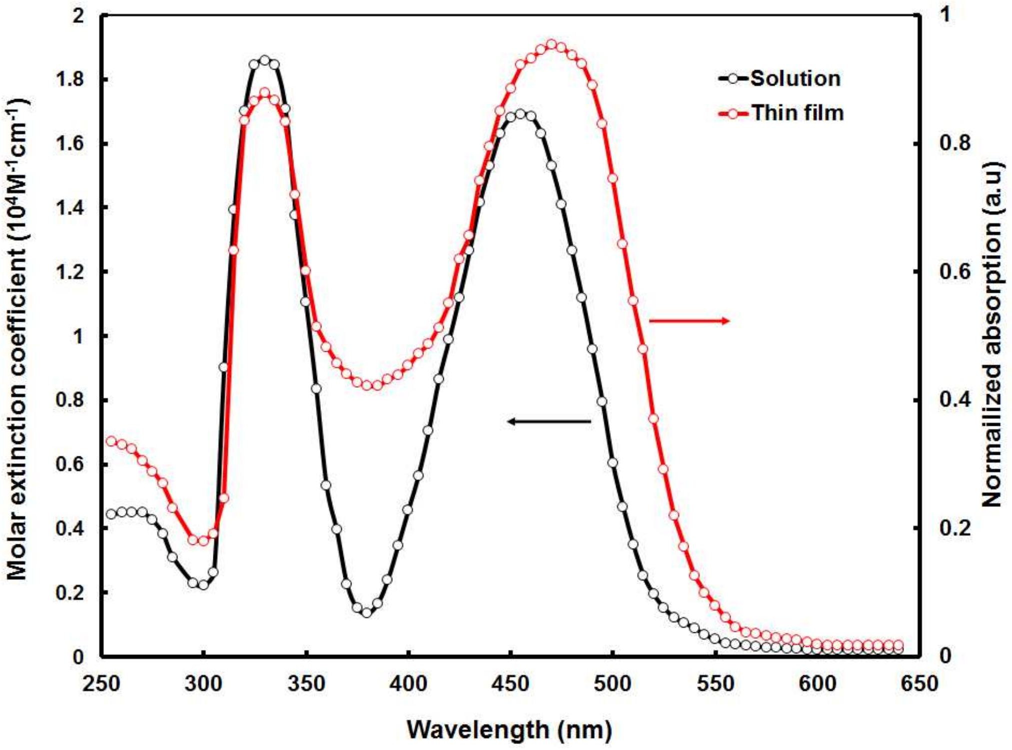

Figure 1: Optical absorption spectra of **CSORG5** in solution and thin film

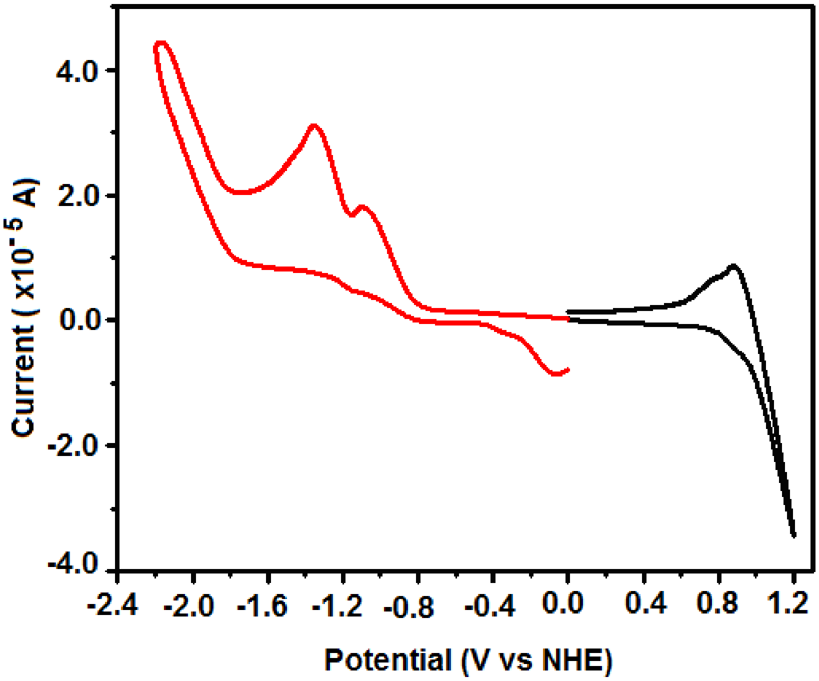

Figure 2: Cyclic voltammogram of **CSORG5**

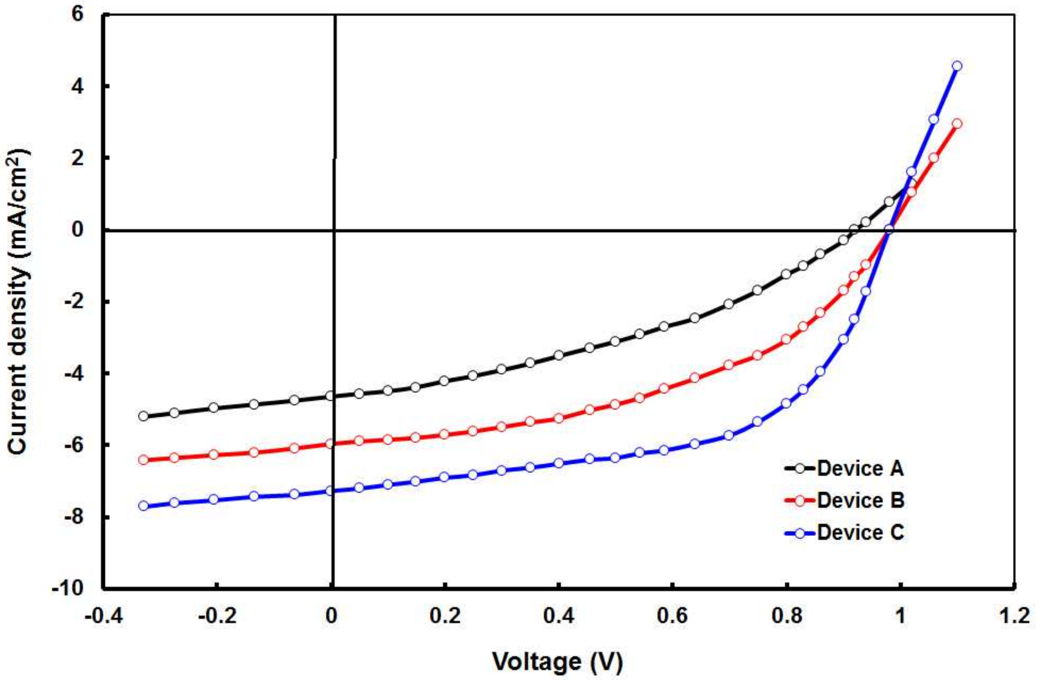

Figure 3: Current –voltage characteristics under illumination (100 mW/cm^2) spectra of the devices

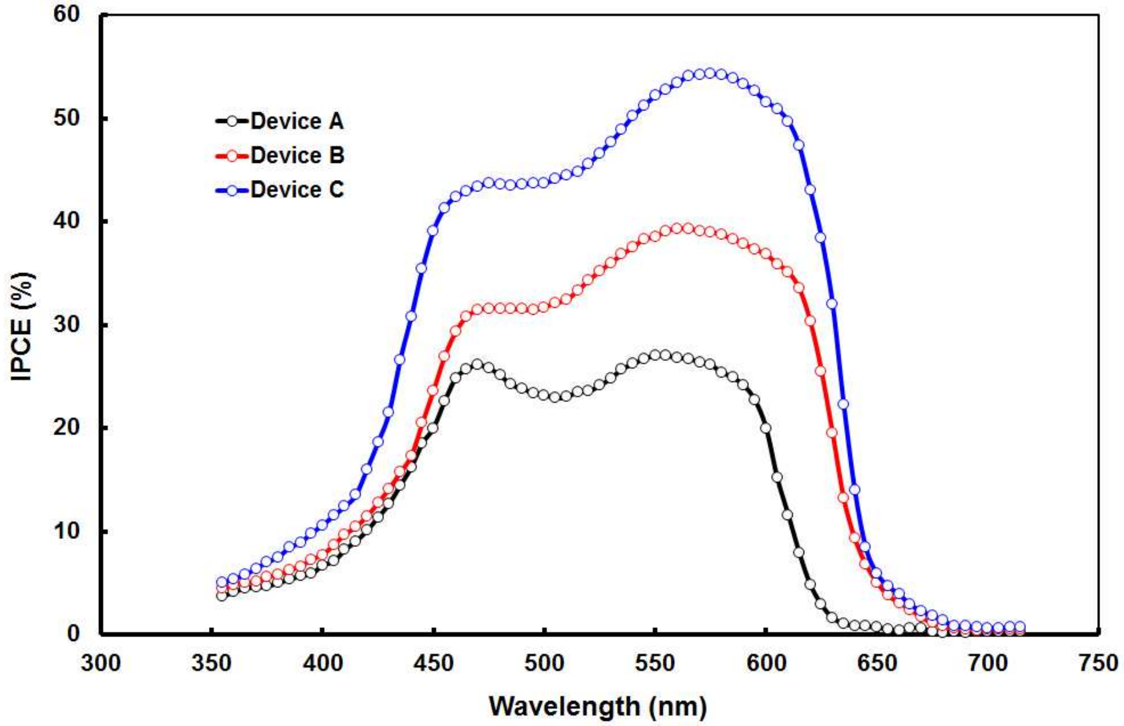

Figure 4: Incident photon to current efficiency (IPCE) spectra of the devices

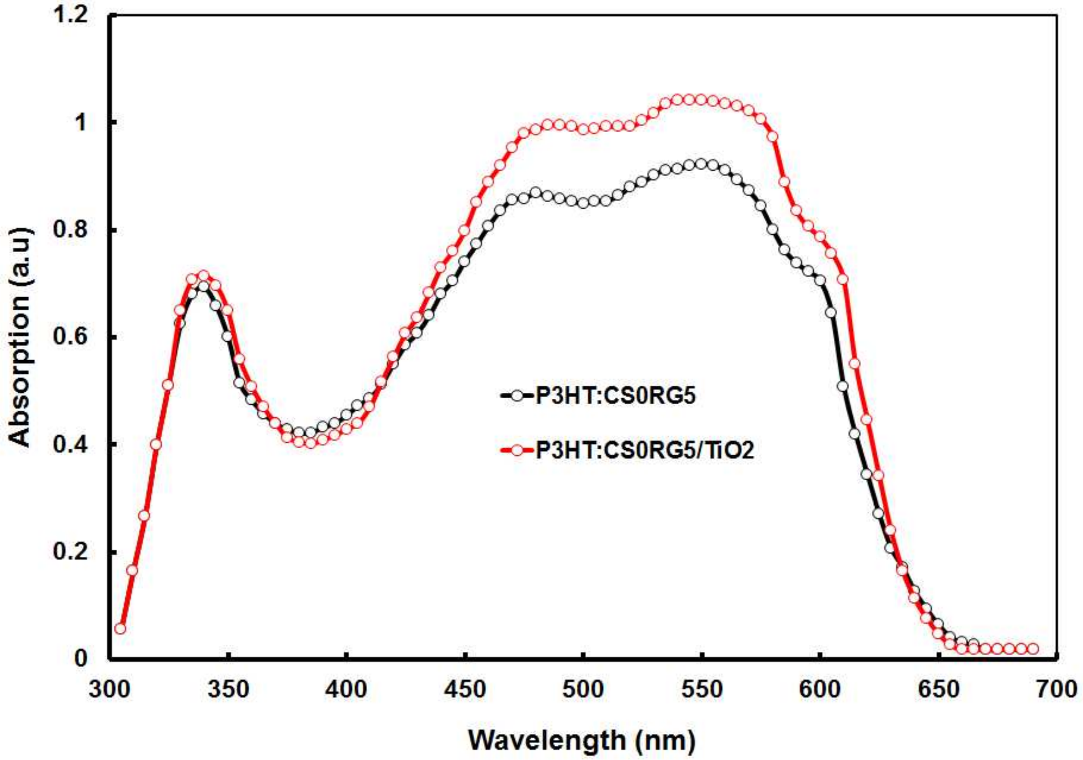

Figure 5: Absorption spectra of P3HT:CSORG5 and P3HT:CSORG5/TiO_2

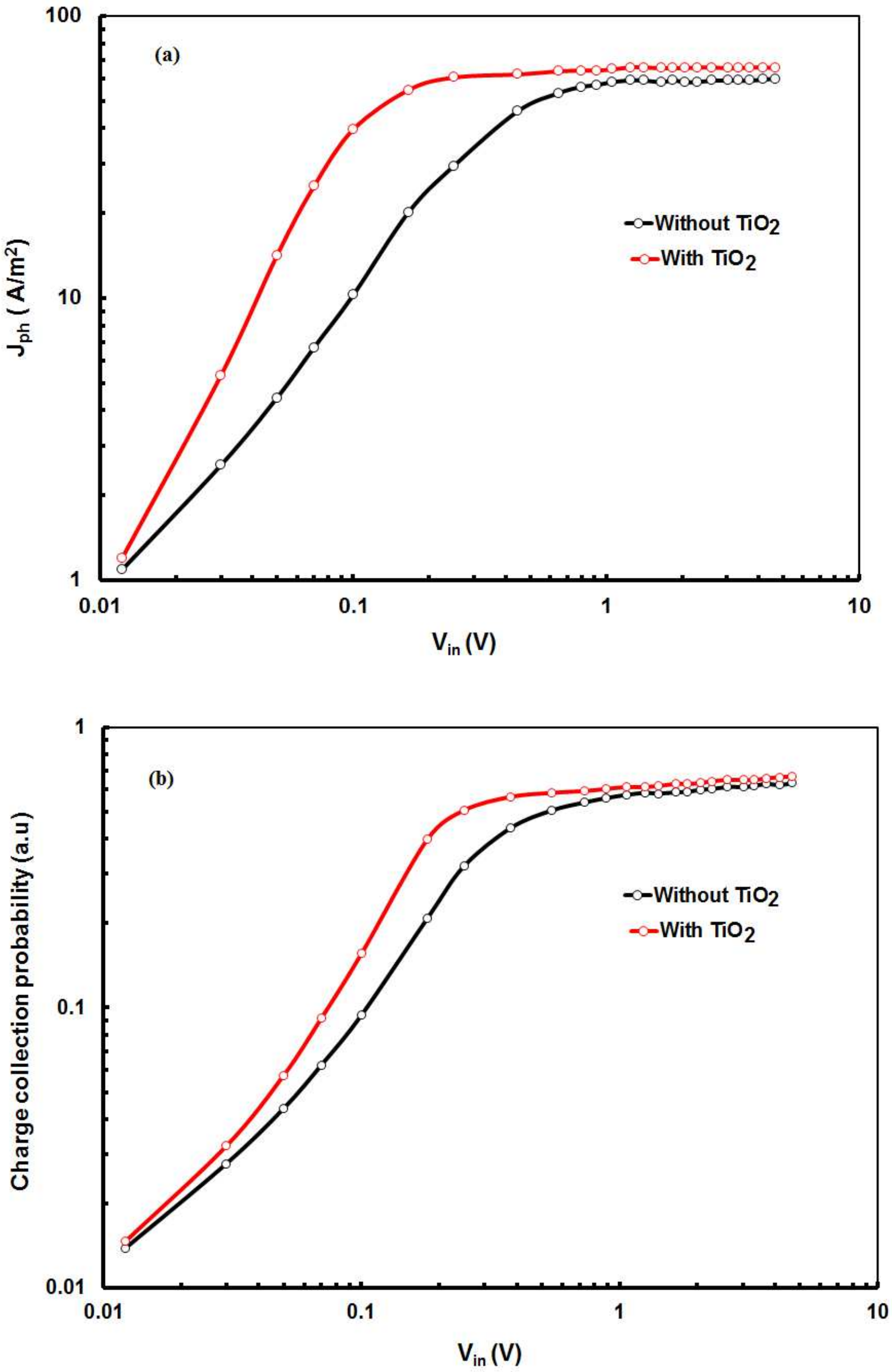

Figure 6: (a) Variation of J_{ph} and (b) charge collection probability (or) normalized photocurrent with saturated photocurrent with internal voltage V_{in} for the device B (without TiO_2) and device C (with TiO_2)

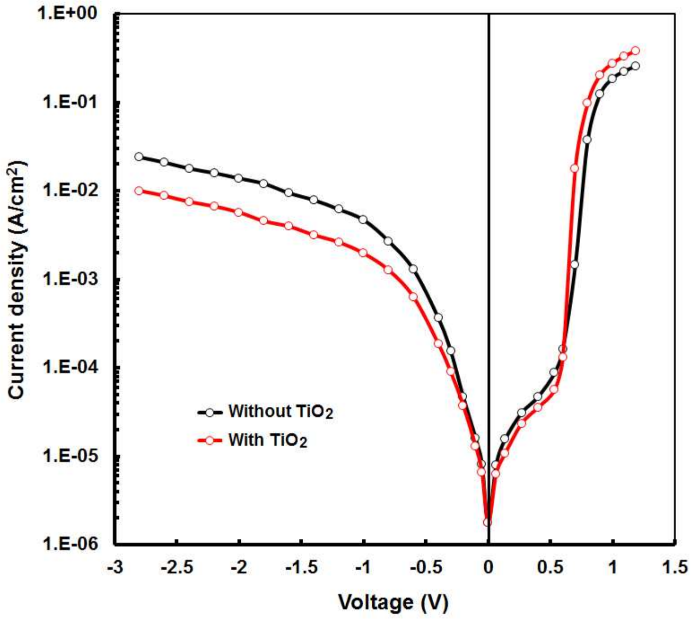

Figure 7: Current-voltage characteristics of device B (without TiO_2) and device C (with TiO_2) in dark

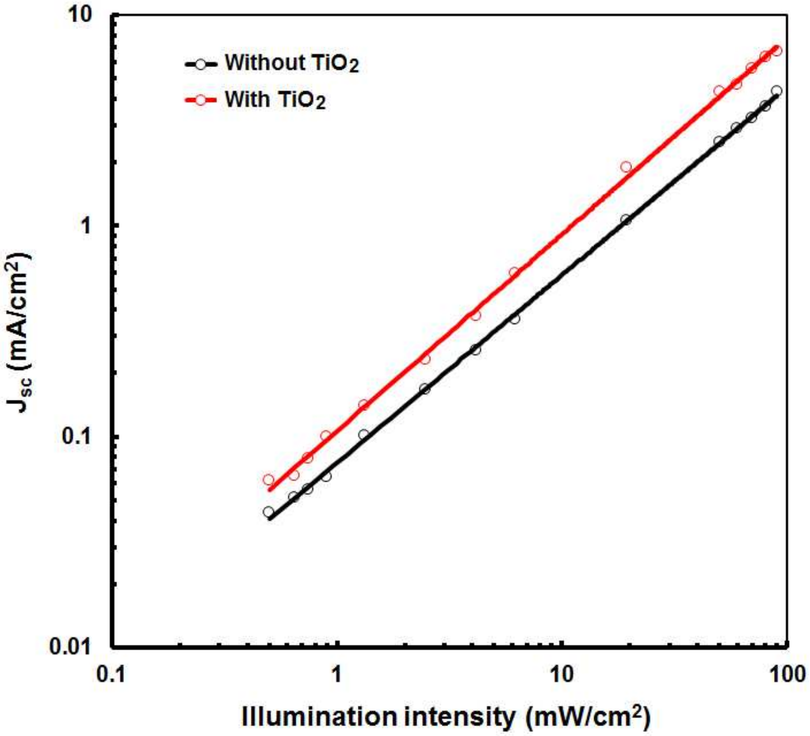

Figure 8: Dependence of J_{sc} with illumination intensity for device B (without TiO_2) and C (with TiO_2)

Graphical Abstract

A novel carbazole-phenothiazine dyad small molecule as non-fullerene electron acceptor for polymer bulk heterojunction solar cells

G. D. Sharma, M. Anil Reddy, D. V. Ramana and M. Chandrasekharam

A small organic molecule **CSORG**5 developed as non-fullerene acceptor for bulk heterojunction solar cells. The device based on P3HT:**CSORG**5 (1:1) spin coated from DIO/THF showed high PCE 2.80% compared to spin coated from THF. The PCE has been further increased to 4.16%, when the thin film TiO_2 was inserted between the active layer and Al electrode.